Construction of a Competing Endogenous RNA Network and Identification of Potential Regulatory Axes in Gastric Cancer Chemoresistance

Xian-Zi Yang
Guangzhou Medical University Affiliated Cancer Hospital
Lei Ma
Guangzhou Medical University Affiliated Cancer Hospital
Shu-Xian Fang
Guangzhou Medical University Affiliated Cancer Hospital
Ye Song
Guangzhou Medical University Affiliated Cancer Hospital
Si-Yu Zhu
Guangzhou Medical University Affiliated Cancer Hospital
Chuan Jin
Guangzhou Medical University Affiliated Cancer Hospital
Wei Liu
Guangzhou Medical University Affiliated Cancer Hospital
Qin Lu
Guangzhou Medical University Affiliated Cancer Hospital
Li-Si Zeng
Guangzhou Medical University Affiliated Cancer Hospital
Shu-Zhong Cui (cuishuzhong@gzhmu.edu.cn)
Affiliated Cancer Hospital & Institute of Guangzhou Medical University https://orcid.org/0000-0003-2178-8741

Research

Keywords: gastric cancer, cisplatin, chemoresistance, ceRNA network, ncRNAs

Posted Date: August 10th, 2021

DOI: https://doi.org/10.21203/rs.3.rs-779155/v1

Version of Record: A version of this preprint was published at Pathology - Research and Practice on April 1st, 2022. See the published version at https://doi.org/10.1016/j.prp.2022.153904.

Abstract

Background: The development of chemoresistance is one of the leading causes of chemotherapy failure in gastric cancer (GC). Emerging evidence highlights the multifunctional role of noncoding RNAs (ncRNAs) in GC chemoresistance. However, the comprehensive expression profile and competing endogenous RNAs (ceRNAs) regulatory network between ncRNAs and mRNAs in GC chemoresistance remain unanswered.

Methods: GC cell line MGC-803 was employed to create cisplatin-resistant MGC-803/DDP cells by continuous exposure to increasing doses of cisplatin. The whole-transcriptome sequencing (RNA sequencing) was performed to comprehensively analyze the differentially expressed (DE) lncRNAs, miRNAs and mRNAs in MGC-803/DDP and MGC-803 cells. Gene Ontology (GO) and Kyoto Encyclopedia of Genes and Genomes (KEGG) pathway enrichment analyses were conducted to investigate the biological functions implicated with the DEncRNAs. Then, the cisplatin-resistant-related ceRNA network and potential regulatory axes were constructed by bioinformatic analysis.

Results: We successfully generated cisplatin-resistant GC cell line MGC-803/DDP. Differential expression analysis showed that a total of 1,936 DElncRNAs, 2,194 DEmRNAs and 174 DEmiRNAs were identified. Functional enrichment analysis indicated that those DEncRNAs were mainly involved in neuroactive ligand-receptor interaction, drug metabolism, Hippo signaling pathway, cAMP pathway and P53 pathway. Subsequently, the cisplatin-resistant-related ceRNA network consisting of 71 DElncRNAs, 121 DEmRNAs and 8 DEmiRNAs was constructed with the widely accepted vital chemo-resistant-related genes and signaling pathways. In addition, two constructed regulatory axes (include FAM66C/miR-129-5p/7 mRNAs and SFTA1P/miR-206/FN1 or NRP1) were successfully validated by the Genomic Data Commons (GDC) GC data.

Conclusion: Our study has shown that differentially expressed ncRNAs have complex and intricate interactions in the cisplatin resistance of GC. The novel ceRNA network and the potential regulatory axes may provide the most comprehensive view of GC chemoresistance to date. Our findings uncovered potential biomarkers for prognostic prediction and novel therapeutic targets for reversing cisplatin resistance in GC.

Background

Gastric cancer (GC) is emerging as the fifth most common cancer and the fourth leading cause of cancer-related death globally [1]. First-line systemic therapy regimens of advanced GC patients include fluorouracil combined with either oxaliplatin or cisplatin (DDP) [2]. However, the 5-year overall survival (OS) of GC patients with local and distant metastasis is rather low [3]. The poor prognosis is due to multiple factors, including chemotherapy resistance, which becomes the most common cause of treatment failure [4]. In the last few decades, many studies have convincingly shown that genetic

alterations, such as DNA methylation, and epigenetic changes, such as ectopic expression of noncoding RNAs (ncRNAs) exert critical roles in the development of chemoresistance in GC [5, 6].

Noncoding RNAs (ncRNAs) is RNA transcripts lacking protein-coding capacity and are classified as small ncRNAs (sncRNAs, < 200 nt), such as microRNAs (miRNAs), small nuclear RNAs (snRNAs), piwi interacting RNAs (piRNAs) and small nuclear RNAs (snoRNAs), and long noncoding RNAs (lncRNAs, > 200 nt) [7]. Besides, circular RNAs (circRNAs) are identified as a new type of lncRNA with the special ring structure [8]. With the development of high-throughput next-generation sequencing (NGS) technologies, extensive published evidence has deepened our understanding of the role of ncRNAs in cancer progression including proliferation, metastasis, apoptosis and chemoresistance [9]. In gastric cancer, Hu et al have reported that MALAT1 expression was upregulated in chemo-resistant GC cells. MALAT1 functioned as a sponge of miR-23b-3p to downregulate ATG12 expression and promoted chemo-induced autophagy and chemoresistance in GC [10]. Li et al have shown that miR-148a-3p sensitized DDP-resistant GC cells to DDP by promoting mitochondrial fission-induced apoptosis and inhibiting autophagosome formation [11]. Similarly, circAKT3 (has_circ_0000199), enhanced DNA damage repair and inhibited the apoptotic capacity of DDP-resistant GC cells by regulating the miR-198/PIK3R1 pathway [12]. Therefore, these competing endogenous RNAs (ceRNAs) regulatory patterns, including lncRNA-miRNA-mRNA and circRNA-miRNA-mRNA, constitute critical contributors to the mechanism of GC chemo-resistance.

Recently, construction and analysis of lncRNA-mediated ceRNA network have been indicated to provide a novel way to delineate the transcriptomic landscape of tumor development (including chemo-resistance) and identify new ncRNAs as potential biomarkers and therapeutic targets for many cancers [13–15]. For example, Zhang et al have successfully constructed a ceRNA network related to FOLFOX chemoresistance in metastatic colorectal cancer (mCRC). A risk factor model based on the hub lncRNAs was constructed to predict FOLFOX chemoresistance and prognosis of mCRC patients [16]. Xiong et al also constructed a chemoresistance-related lncRNA-associated ceRNA network of pancreatic cancer (PC). Using bioinformatic analyses, GSTM3TV2 was identified as a key regulator of chemoresistance, which promoted PC cells gemcitabine resistance [17]. However, the comprehensive expression profile of a cisplatin-resistant-related ceRNA regulatory network and identified key regulators of the ceRNA network in GC has not been reported to date.

Herein, whole-transcriptome sequencing (RNA sequencing) was performed to screen differentially expressed (DE) lncRNAs, miRNAs and mRNAs potential involved in DDP resistance by using two chemo-resistant GC cell lines (MGC-803/DDP versus MGC-803 cells). To explore the main functional pathway of GC chemoresistance, DEmRNAs were evaluated by Kyoto Encyclopedia of Genes and Genomes (KEGG) and Gene Ontology (GO) annotation. Then we constructed the cisplatin-resistant-related lncRNA-associated ceRNA network by functional interaction prediction analysis. Finally, two constructed ceRNA regulatory pathways were selected and validated by The Cancer Genome Atlas (TCGA) GC database. This study may provide a comprehensive view of GC chemoresistance based on the construction of cisplatin-resistant-related ceRNA network, and discover some potential therapeutic targets for reversing it.

Materials And Methods

Cell lines and culture

The human GC cell line MGC-803 was purchased from the Cell Bank of the Chinese Academy of Science (Shanghai, China) and cultured in RPMI-1640 supplemented with 10% fetal bovine serum (FBS, Hyclone, Logan, UT, USA) at 37°C with an atmosphere of 5% CO_2. Cisplatin-resistant MGC-803 cells (MGC-803/DDP) were established by our laboratory. Briefly, MGC-803 cells were initially exposed to 0.03 μM of DDP for 2 weeks. The drug concentration was intermittently increased up to 3.33 μM over one year. To maintain the chemoresistant phenotype, MGC-803/DDP cells were cultured in complete culture medium with 1.67 μmol/L DDP. These two GC cells were stored in liquid nitrogen for further experiments. The complete experiment workflow is shown in Fig. 1.

The half-maximal inhibitory concentration (IC50) analysis by CCK8 assay

For cisplatin IC50 analysis, MGC-803 and MGC-803/DDP cells were seeded into 96-well plates and treated with the indicated concentration of cisplatin for 48 hours. 10 μl Cell Counting Kit-8 (CCK-8) solution (Dojindo, Tokyo, Japan) was added to each well. After 2 hours of incubation at 37 ℃, the optical density (OD) values were measured at a wavelength of 450 nm by Thermo Scientific Varioskan Flash (Thermo Fisher Scientific, USA). Cell growth inhibition rates were described as cell inhibiting curves and The IC50 parameters were calculated by GraphPad Prism V8 (GraphPad Prism, Inc., La Jolla, CA, USA).

RNA extraction, quality control, library construction and microarray analysis

Total RNA from MGC-803 and MGC-803/DDP cells was isolated using TRIzol reagent (Life Technologies, CA, USA) according to the manufacture's instruction. The RNA concentration and quality were assessed with the Agilent Bioanalyzer 2100 system (Agilent Technologies, CA, USA). All RNA samples had an RNA Integrity Number (RIN) > 8.0. RNA-seq was assessed to identify the differentially expressed (DE) lncRNAs, mRNAs and miRNAs in MGC-803 and MGC-803/DDP cells. NEBNext® Ultra™ II RNA Library Prep Kit for Illumina® (NEB, USA) was used with 2 μg of total RNA for the construction of sequencing libraries on the Illumina NovaSeq 6000-sequencing platform (Tsingke Biotechnology Co. Ltd, Beijing, China). The raw reads were filtered and cleaned by removing the adaptor reads and low-quality tags. Then clean paired-end reads were aligned to the reference genome using HISAT2 (v2.0.4) for transcripts and Bowite (v2.2.5) for miRNA as described [18, 19]. Subsequently, raw counts were generated by the StringTie (v.2.1.2) for transcripts and the FeatureCounts (v1.6.1) for miRNAs [20, 21].

Identification of DERNAs

To screen the DE lncRNAs, miRNAs and mRNAs in MGC-803/DDP in comparison with MGC-803 cells, the expression profiles were analyzed using the edgeR package [22] installed in R (version 4.0.5, www. r-project. org). Fold change (log_2 absolute) ≥ 2 were considered as the thresholds for identifying DERNAs. Heatmaps were drawn using the "pheatmap" R packages to show DERNAs.

Functional annotation and pathway enrichment of the DEmRNAs

To investigate the biological functions implicated with the DEmRNAs, Kyoto Encyclopedia of Genes and Genomes (KEGG) pathway analysis and Gene Ontology (GO) functional analysis were performed using the commonly used online database DAVID [23] (version 6.8; https://davidd. ncifcrf.gov/). The Gene Ontology Biological Process (GO-BP) term and pathway with the enriched gene count ≥ 2 and the significance threshold $P < 0.05$ were considered significant. The top 20 significant biological processes or pathways were visualized by Bubble maps created by "ggplot2" package in R software.

Construction of protein-protein interaction (PPI) network of DEmRNAs

The PPI network of DEmRNAs was constructed by the Search Tool for the Retrieval of Interacting Genes (STRING, version 11.0; https://string-db.org/cgi/input.pl). The input gene set was set as all DEmRNAs, and the species was set as homo sapiens. The minimum required interaction score was set as the highest confidence (0.900). The PPI network was visualized by Cytoscape software (version 3.8.2; https://cytoscape.org/). The CytoNCA plug-in in Cytoscape software was implemented to determine the network topology properties of the nodes, and the parameters were set as "without weight". We used the MCODE plug-in in Cytoscape software to analyze functionally related and highly interconnected modules from the PPI network with the threshold score ≥ 12. Then hub genes from the significant clustering modules were subjected to KEGG pathway analysis with the enriched gene count ≥ 2 and the significance threshold $P < 0.05$ as the cut-off criterion.

Prediction of DEmiRNAs regulatory relationship

The miRNA-lncRNA regulatory relationship of DEmRNAs was predicted using the miRcode database (http://www.mircode.org/). The predicted miRNA-lncRNA regulatory relationship was integrated with DElcnRNAs and DEmiRNAs to obtain the DEmiRNA-DElncRNA relationship. In the light of this regulatory relationship, these screened DEmiRNAs were further used to predict the miRNA-mRNA regulatory relationship via four publicly profile datasets (TargetScan, miRDB, miRTarbase and ENCORI). The screening criteria were the number of supporting datasets ≥ 3. The predicted miRNA-mRNA regulatory relationship was integrated with DEmRNAs to obtain the DEmiRNA-DEmRNA relationship.

KEGG pathway analysis of DEmiRNAs and DElncRNAs

Based on the obtained DEmiRNA-DElncRNA and DEmiRNA-DEmRNA regulatory relationships and the co-expression relationship between DEmRNAs and DElncRNAs, the compareCluster function in the clusterProfiler package (http://bioconductor.org/ packages/release/bioc/html/clusterProfiler.html) in R software was performed to calculate and compare KEGG pathway enrichment analysis of screened DEmiRNAs and DElncRNAs. The pathway with the threshold $P < 0.05$ was considered significant. Bubble maps are implemented to indicate pathways in which DEmiRNAs and DElncRNAs may be implicated.

Construction of the ceRNA regulatory network

According to the ceRNA hypothesis, lncRNAs can function as decoys for various miRNAs and modulate target genes' stability or translation [23]. We used the obtained DEmiRNA-DElncRNA and DEmiRNA-DEmRNA regulatory relationships and the correlation coexpression of DElncRNA-mRNA pairs to construct a lncRNA-miRNA-mRNA regulatory network. Because DEmiRNAs expression was negatively associated with DElncRNAs or DEmRNAs based on the ceRNA hypothesis, the positive correlation expression of DEmiRNA-DElncRNA pairs and DEmiRNA-DEmRNA pairs were excluded from our ceRNA network. We conducted the Cytoscape software (version 3.8.2) to visualize the ceRNA network, and the cytoHubba plug-in was implemented to rank nodes by their network features and select the top 50 genes from maximal clique centrality (MCC) as the hub genes [24]. To screen potential ceRNA regulatory axes, R package "ggalluvial" and "ggplot2" were performed to identify the ceRNA axes.

GDC GC data validation and identification of prognostic predictors

For data validation, the RNA-seq and miRNA expression profiles and clinical information of gastric cancer were downloaded from the Genomic Data Commons (GDC) data portal (https://gdc.xenahubs.net). The lncRNAs and mRNAs data contained 343 GC tissues and 30 matched non-cancerous tissues, and the miRNAs data included 410 GC samples and 42 adjacent cancer normal samples. The differentially expressed lncRNAs, mRNAs and miRNAs between GC and normal tissues were screened out using the edgeR package (http://bioconductor.org/packages/edgeR/) in R software [22]. The survival package was applied to explore the prognostic value of DElncRNAs, DEmiRNAs and DEmRNAs in the ceRNA network, with clinical data of GDC combined. This test is based on the Kaplan-Meier method and P value < 0.05 was considered statistically significant. Regression analysis was performed to detect the correlation between DElncRNAs and DEmRNAs expression from GDC GC data with $P < 0.01$ and $r > 0.3$ as the criteria for significance.

Statistical analysis

All statistical analyses were conducted using SPSS 24.0 (SPSS, Chicago, IL, USA), GraphPad Prism V8 (GraphPad Prism, Inc., La Jolla, CA, USA) and R software (version 4.0.5). Data are presented as the mean ± SEM. The two-tailed Student's t-test and one-way ANOVA analysis were used to compare the different expression levels between two groups. Pearson correlation analysis was performed to evaluate the ceRNA network construction. The Kaplan-Meier method and log-rank test were employed to generate the survival curve and compare differences between survival curves, respectively. A P value < 0.05 was considered statistically significant.

Results

Identification of cisplatin-resistant-related differentially expressed lncRNAs, miRNAs and mRNAs

After continuous exposure to increasing concentration of cisplatin for one year, we successfully generated cisplatin-resistant GC cell line MGC-803/DDP. The IC50 values for MGC-803 and MGC-803/DDP cells were 0.86 μmol/L and 24.21 μmol/L, respectively (Fig. 2a). The whole-transcriptome sequencing

data (lncRNAs, mRNAs and miRNAs) was acquired from MGC-803 and MGC-803/DDP cells by the Illumina NovaSeq 6000-sequencing platform. According to the screening criteria, a total of 1,936 DElncRNAs were obtained, of which 1,006 were upregulated and 930 were downregulated; 2,194 DEmRNAs were identified, including 1,427 were upregulated and 767 were downregulated; 174 DEmiRNAs were obtained, of which 83 were upregulated and 91 were downregulated. DElncRNAs, DEmiRNAs and DEmRNAs in the samples were indicated using the two-way clustering heatmaps (Fig. 2b-d). Thus, we suggest that these different expressions of RNAs may lead to the chemoresistance of GC, and further analysis is necessary to better understand the regulatory relationship among these DERNAs.

GO functional enrichment and KEGG pathway analysis of DEmRNAs

GO enrichment and KEGG pathway analysis were conducted to evaluate the biological effects of up and down-regulated DEmRNAs individually. The results showed that the upregulated DEmRNAs were enriched in 152 Gene Ontology Biological Process (GO-BP) terms, whereas the downregulated DEmRNAs were enriched in 55 GO-BP terms. We evaluated the top 20 significant GO-BP terms enriched in DEmRNAs associated with DDP resistance (Fig. 3a-b). The upregulated genes were mainly enriched in inflammatory response, defense response to virus, cell adhesion and chemotaxis (Fig. 3a), whereas the downregulated genes were related to the regulation of calcium ion-dependent exocytosis, positive regulation of ERK1 and ERK2 cascade, negative regulation of angiogenesis and positive regulation of Rho protein signal transduction (Fig. 3b). KEGG pathway analysis revealed that the upregulated genes were remarkably involved in neuroactive ligand-receptor interaction, hematopoietic cell lineage, cytokine-cytokine receptor interaction and cell adhesion molecules (CAMs) (Fig. 3c), but the downregulated genes were associated with biosynthesis of amino acids, cytokine-cytokine receptor interaction, complement and coagulation cascades, and neuroactive ligand-receptor interaction (Fig. 3d). Therefore, our findings might foreshadow the complexity yet to be uncovered regarding the cisplatin resistance in gastric cancer.

Protein-protein interaction (PPI) network construction and module extraction

The cisplatin-resistant-related PPI network was constructed using all DEmRNAs. After removing disconnected nodes, the PPI network consisted of 1888 nodes and 3750 edges. To investigate the significant modules in the process of GC chemoresistance, the MCODE plug-in (score ≥ 12) was used and seven highly interconnected modules were subsequently extracted from the PPI network (Fig. 4a-b). Module 1 (score = 43.86) contained 44 nodes and 943 edges, including growth-regulated α protein (CXCL1), guanine nucleotide-binding protein subunit γ-T2 (GNGT2), kininogen-1 (KNG1) and sphingosine 1-phosphate receptor 1 (S1PR1). Module 2 (score = 24) contained 24 nodes and 276 edges, including platelet-activating factor receptor (PTAFR) and substance-P receptor (TACR1). Module 3 (score = 19) contained 19 nodes and 171 edges, including Fibronectin 1 (FN1) and Glypican-3 (GPC3). Module 4 (score = 16.5) contained 33 nodes and 264 edges, including E3 ubiquitin-protein ligase CBL-B (CBLB), 2’-5’-oligoadenylate synthase-like protein (OASL) and Radical S-adenosyl methionine domain-containing protein 2 (RSAD2). Module 5 (score = 13) contained 13 nodes and 78 edges, including neutrophil collagenase (MMP8) and Aldolase fructose-bisphosphate C (ALDOC). Module 6 (score = 12) contained 12 nodes and 66 edges, including G-protein coupled receptor 84 (GPR84), glycoprotein hormones α

polypeptide (CGA) and 5-hydroxytryptamine receptor 7 (HTR7). Module 7 (score = 12) contained 12 nodes and 66 edges, in which the genes belong to the keratin protein family, such as keratin type I cytoskeletal 13 (KRT13), keratin type II cytoskeletal 2 epidermal (KRT2) and keratin type I cuticular Ha2 (KRT32).

We further explored crucial signaling pathways of genes in the abovementioned modules using KEGG pathway enrichment analyses. The results showed that 18 remarkable enriched pathways might be related to GC chemoresistance (Fig. 4c). The top four significant pathways were neuroactive ligand-receptor interaction, calcium signaling pathway, chemokine signaling pathway and cytokine-cytokine receptor interaction. Taken together, these data suggest that many proteins and related signaling pathways are involved in the cisplatin resistance of GC cells.

KEGG pathway enrichment analysis of DEmiRNAs and DElncRNAs-related target genes

Integrated bioinformatic analysis revealed that the DEmiRNA-DElncRNA regulatory relationship consisted of 8 DEmiRNAs and 102 DElncRNAs, and the DEmiRNA-DEmRNA relationship contained 8 DEmiRNAs and 200 DEmRNAs (Fig. 5a). According to the above two regulatory relationships and the co-expression relationship between DEmRNAs and DElncRNAs, R package “clusterProfiler” was performed and the results were shown by bubble maps. Figure 5b and Fig. 5c displayed only the top 20 pathways enriched by those genes related to DEmiRNAs and DElncRNAs. From the results, we found that the DEmiRNAs-related genes were significantly enriched in neuroactive ligand-receptor interaction, drug metabolism, Hippo signaling pathway and cAMP signaling pathway. Additionally, the DElncRNAs-related genes were striking involved in axon guidance, neurotrophin signaling pathway and P53 signaling pathway. Collectively, these results indicated that these screened DEmiRNAs and DElncRNAs-related pathways (mainly nerve conduction and metabolic pathway) play important roles in GC chemoresistance.

Construction of cisplatin-resistant-related ceRNA network

The above results were integrated to construct the cisplatin-resistant-related ceRNA network. This network comprised 199 nodes (71 DElncRNAs, 121 DEmRNAs and 8 DEmiRNAs) and 227 interactions (Fig. 6a-b). We noted that 5 DElncRNAs, including LINC00200 [25], LINC00460 [26], MEG3 [27], NEAT1 [28] and UCA1 [29], have been substantiated to be chemoresistant-related genes. Interestingly, some studies have also reported that MEG3, NEAT1 and UCA1 exerted vital roles in regulating cisplatin resistance in ovarian cancer [30], lung cancer [31] and gastric cancer [32]. Moreover, we selected the top 50 interactomes from this ceRNA network to construct cisplatin-resistant-related regulatory axes which consist of 22 DElncRNAs, 7 DEmiRNAs and 21 DEmRNAs (Fig. 6c). Therefore, this specific ceRNA network may provide the missing piece of the well-known chemoresistant-related network puzzle in GC.

Prognostic value of DERNAs from GDC GC dataset and identification of potential regulatory axes

The prognostic value of DERNAs from the ceRNA network was analyzed to discover the prognostic factors according to the sequencing data from GDC gastric cancer samples. As shown in Fig. 7, 4 DElncRNAs and 19 DEmRNAs were identified as oncogenes because high expression of these DERNAs

was positively associated with poor prognosis of GC patients ($P < 0.05$). We further analyzed the correlation between the abovementioned 4 DElncRNAs and 19 DEmRNAs based on GDC GC data. The results indicated that the expression of FAM66C was significant correlated with those of seven DEmRNAs (EBF3, EDA2R, FBXL2, RUNDC3B, SEMA3E, SLC16A7 and VCAN) ($r > 0.3$, $P < 0.01$) (Fig. 8a). And lncRNA SFTA1P expression was also positively correlated with those of FN1 and NRP1 ($r > 0.3$, $P < 0.01$) (Fig. 8b). Based on the hypothesis of ceRNA and the above findings, we identified two potential regulatory axes from the cisplatin-resistant-related ceRNA network, which include FAM66C/miR-129-5p/7 mRNAs and SFTA1P/miR-206/FN1 or NRP1 (Fig. 8c). Therefore, these two potential regulatory axes may exert important roles in GC chemoresistance.

Discussion

Currently, platinum-based chemotherapy is the preferred treatment for gastric cancer patients by their specific anticancer properties and extensive anticancer spectrum [2]. However, most GC patients will inevitably and eventually relapse and metastases with chemo-resistant diseases, which result in treatment failure and poor outcome [33]. In recent years, multiple ncRNAs have been demonstrated to play critical roles in the chemoresistance of GC, including cisplatin resistance [6]. But the majority of these studies focused on the role of individual ncRNAs in GC chemoresistance, which neglected the complexity and diversity of the gene regulatory network. Thanks to the rapid development of NGS sequencing technologies and bioinformatics, we used this effective method to identify the relationship between networks/genes, pathways and clinical characteristics to avoid the defects of the traditional method [34, 35]. In this study, we identified 1,936 DElncRNAs, 2,194 DEmRNAs and 174 DEmiRNAs in one paired cisplatin-resistant GC cell lines by the whole-transcriptome RNA-sequencing. Functional enrichment analysis showed that DEmRNAs were mainly involved in neuroactive ligand-receptor interaction, cytokine-cytokine receptor interaction, chemokine signaling pathway and CAMs. The enrichment analysis of DEmiRNA and DElncRNAs-related target genes further indicated that these genes were enriched in neuroactive ligand-receptor interaction, drug metabolism, Hippo signaling pathway, cAMP pathway and P53 pathway.

To the best of our knowledge, several lines of evidence have supported the ceRNA hypothesis that many ncRNAs can regulate mRNA stability or translation and modulate carcinogenesis by acting as decoys for miRNAs or miRNA “sponges” [36]. Although the ceRNA regulatory networks were intricate and complex, they can be implemented to provide a more comprehensive view of the RNA regulatory mechanism in cancer chemoresistance [37]. Actually, Wu et al. [38] constructed a lung adenocarcinoma-specific ceRNA network based on differentially expressed lncRNAs, miRNAs and mRNAs from TCGA data portal. Pan et al. [13] showed the interactions of lncRNAs, miRNAs and mRNAs to reveal a novel ceRNA network and the potential regulatory axes in GC. However, the question on the comprehensive analysis of differentially expressed profiles of lncRNAs and ceRNA networks in GC chemoresistance still begs an answer. In the present study, we successfully constructed the cisplatin-resistant-related ceRNA network including 71 DElncRNAs, 121 DEmRNAs and 8 DEmiRNAs. The selected ncRNAs in this network conformed to the ceRNA rules and some of them were demonstrated to be well-established drug-resistant-related genes or

signaling pathways in many cancers [25–32]. Therefore, this network provided a credible and systematic perspective on the potential function of lncRNAs in cisplatin resistance of GC.

To determine the prognostic value of our cisplatin-resistant-related ceRNA network, we selected GDC GC database for validation. Prognostic analysis and regression analysis showed that two regulatory axes (include FAM66C/miR-129-5p/7 mRNAs and SFTA1P/miR-206/FN1 or NRP1) were identified to be hub genes and might be adapted to predict the cisplatin-based chemotherapy response.

Several limitations need to be mentioned. First, this study subject is GC cell lines, not GC samples. But the publicly available dataset (TCGA or GDC) which contains many GC tissues and matched normal tissues was used to verify our findings. Second, the enrichment analysis of hub genes was conducted by whole-transcriptome profiling and bioinformatics analysis. We intend to further validate these predictive results by experimental studies in the future.

Conclusion

In summary, this study is the first report analyzing the differential expression of lncRNAs, miRNAs, and mRNAs in the GC chemoresistance using whole-transcriptome RNA-sequencing and through validation by GDC data. The cisplatin-resistant-related ceRNA network and regulatory axes were constructed to reveal the underlying mechanism of the cisplatin resistance of GC. Our findings narrow the scope of research and improve the predictive accuracy for target lncRNAs or mRNAs, and the latter may serve as promising biomarkers for predicting chemotherapy response and prognosis and therapeutic targets of GC patients.

Abbreviations

GC: Gastric cancer; ncRNAs: Noncoding RNAs; ceRNAs: Competing endogenous RNAs; DDP: cisplatin; DE: Differentially expressed; GO: Gene Ontology; KEGG: Kyoto Encyclopedia of Genes and Genomes; GDC: Genomic Data Commons; OS: overall survival; miRNAs: microRNAs; circRNAs: circular RNAs; NGS: next-generation sequencing; mCRC: metastatic colorectal cancer; PC: pancreatic cancer; TCGA: The Cancer Genome Atlas; CCK-8: Cell Counting Kit-8; OD: optical density; RIN: RNA Integrity Number; GO-BP: Gene Ontology Biological Process; PPI: protein-protein interaction; MCC: maximal clique centrality; CAMs: cell adhesion molecules.

Declarations

Authors' contributions

SZC, LSZ, and QL designed the study. XZY, LM, YS, and SXF conducted the study and prepared the Figures and tables; XZY, SXF, CJ, WL, and SYZ collected data and performed the statistical analyses; XZY, YS, LSZ, and QL analyzed and interpreted the data; XZY, LSZ, and SZC wrote and revised the manuscript. All authors read and approved the final manuscript.

Funding

This study was supported by grants from the National Natural Science Foundation of China (No.81972918), Guangzhou Key Medical Discipline Construction Project Fund; Guangzhou High-Level Clinical Key Specialty Construction Project (No.2019-2021); Clinical Key Specialty Construction Project of Guangzhou Medical University (YYPT202017).

Availability of data and materials

Because of our internal policy, raw data cannot be shared.

CONFLICTS OF INTEREST

The authors declare no conflict of interest.

Ethics approval and consent to participate

Not applicable.

Consent for publication

Not applicable.

Competing interests

The authors declare that they have no competing interests.

References

1. Sung H, Ferlay J, Siegel RL, Laversanne M, Soerjomataram I, Jemal A, et al. Global cancer statistics 2020: GLOBOCAN estimates of incidence and mortality worldwide for 36 cancers in 185 countries. CA Cancer J Clin. 2021.
2. Smyth EC, Nilsson M, Grabsch HI, van Grieken NC, Lordick F. Gastric cancer. Lancet. 2020;396(10251):635-48.
3. Thrift AP, El-Serag HB. Burden of Gastric Cancer. Clin Gastroenterol Hepatol. 2020;18(3):534-42.
4. Biagioni A, Skalamera I, Peri S, Schiavone N, Cianchi F, Giommoni E, et al. Update on gastric cancer treatments and gene therapies. Cancer Metastasis Rev. 2019;38(3):537-48.
5. Choi SJ, Jung SW, Huh S, Chung YS, Cho H, Kang H. Alteration of DNA Methylation in Gastric Cancer with Chemotherapy. J Microbiol Biotechnol. 2017;27(8):1367-78.
6. Wei L, Sun J, Zhang N, Zheng Y, Wang X, Lv L, et al. Noncoding RNAs in gastric cancer: implications for drug resistance. Mol Cancer. 2020;19(1):62.
7. Beermann J, Piccoli MT, Viereck J, Thum T. Non-coding RNAs in Development and Disease: Background, Mechanisms, and Therapeutic Approaches. Physiol Rev. 2016;96(4):1297-325.

8. Zhang M, Du X. Noncoding RNAs in gastric cancer: Research progress and prospects. World J Gastroenterol. 2016;22(29):6610-8.
9. Cech TR, Steitz JA. The noncoding RNA revolution-trashing old rules to forge new ones. Cell. 2014;157(1):77-94.
10. YiRen H, YingCong Y, Sunwu Y, Keqin L, Xiaochun T, Senrui C, et al. Long noncoding RNA MALAT1 regulates autophagy associated chemoresistance via miR-23b-3p sequestration in gastric cancer. Mol Cancer. 2017;16(1):174.
11. Li B, Wang W, Li Z, Chen Z, Zhi X, Xu J, et al. MicroRNA-148a-3p enhances cisplatin cytotoxicity in gastric cancer through mitochondrial fission induction and cyto-protective autophagy suppression. Cancer Lett. 2017;410:212-27.
12. Huang X, Li Z, Zhang Q, Wang W, Li B, Wang L, et al. Circular RNA AKT3 upregulates PIK3R1 to enhance cisplatin resistance in gastric cancer via miR-198 suppression. Mol Cancer. 2019;18(1):71.
13. Pan H, Guo C, Pan J, Guo D, Song S, Zhou Y, et al. Construction of a Competitive Endogenous RNA Network and Identification of Potential Regulatory Axis in Gastric Cancer. Front Oncol. 2019;9:912.
14. Niu ZS, Wang WH, Dong XN, Tian LM. Role of long noncoding RNA-mediated competing endogenous RNA regulatory network in hepatocellular carcinoma. World J Gastroenterol. 2020;26(29):4240-60.
15. Wang L, Cho KB, Li Y, Tao G, Xie Z, Guo B. Long Noncoding RNA (lncRNA)-Mediated Competing Endogenous RNA Networks Provide Novel Potential Biomarkers and Therapeutic Targets for Colorectal Cancer. Int J Mol Sci. 2019;20(22).
16. Zhang Y, Xu M, Sun Y, Chen Y, Chi P, Xu Z, et al. Identification of LncRNAs Associated With FOLFOX Chemoresistance in mCRC and Construction of a Predictive Model. Front Cell Dev Biol. 2020;8:609832.
17. Xiong G, Liu C, Yang G, Feng M, Xu J, Zhao F, et al. Long noncoding RNA GSTM3TV2 upregulates LAT2 and OLR1 by competitively sponging let-7 to promote gemcitabine resistance in pancreatic cancer. J Hematol Oncol. 2019;12(1):97.
18. Kim D, Langmead B, Salzberg SL. HISAT: a fast spliced aligner with low memory requirements. Nat Methods. 2015;12(4):357-60.
19. Langmead B. Aligning short sequencing reads with Bowtie. Curr Protoc Bioinformatics. 2010;Chapter 11:Unit 11 7.
20. Liao Y, Smyth GK, Shi W. featureCounts: an efficient general purpose program for assigning sequence reads to genomic features. Bioinformatics. 2014;30(7):923-30.
21. Pertea M, Pertea GM, Antonescu CM, Chang TC, Mendell JT, Salzberg SL. StringTie enables improved reconstruction of a transcriptome from RNA-seq reads. Nat Biotechnol. 2015;33(3):290-5.
22. Robinson MD, McCarthy DJ, Smyth GK. edgeR: a Bioconductor package for differential expression analysis of digital gene expression data. Bioinformatics. 2010;26(1):139-40.
23. Yang XZ, Cheng TT, He QJ, Lei ZY, Chi J, Tang Z, et al. LINC01133 as ceRNA inhibits gastric cancer progression by sponging miR-106-3p to regulate APC expression and Wnt/β-cantenin pathway. Mol

Cancer. 2018;17(1):196.
24. Chin CH, Chen SH, Wu HH, Ho CW, Ko MT, Lin CY. cytoHubba: identifying hub objects and sub-networks from complex interactome. BMC Syst Biol. 2014;8 Suppl 4:S11.
25. Lin M, Xu M, Xu Z, Weng Z, Lin B, Lan Y, et al. LINC00200 contributes to the chemoresistance to oxaliplatin of gastric cancer cells via regulating E2F1/RAD51 axis. Hum Cell. 2021;34(4):1163-73.
26. Meng X, Sun W, Yu J, Zhou Y, Gu Y, Han J, et al. LINC00460-miR-149-5p/miR-150-5p-Mutant p53 Feedback Loop Promotes Oxaliplatin Resistance in Colorectal Cancer. Mol Ther Nucleic Acids. 2020;22:1004-15.
27. El-Khazragy N, Mohammed HF, Yassin M, Elghoneimy KK, Bayoumy W, Hewety A, et al. Tissue-based long non-coding RNAs "PVT1, TUG1 and MEG3" signature predicts Cisplatin resistance in ovarian Cancer. Genomics. 2020;112(6):4640-6.
28. Dong P, Xiong Y, Yue J, Xu D, Ihira K, Konno Y, et al. Long noncoding RNA NEAT1 drives aggressive endometrial cancer progression via miR-361-regulated networks involving STAT3 and tumor microenvironment-related genes. J Exp Clin Cancer Res. 2019;38(1):295.
29. Xie W, Chu M, Song G, Zuo Z, Han Z, Chen C, et al. Emerging roles of long noncoding RNAs in chemoresistance of pancreatic cancer. Semin Cancer Biol. 2020.
30. Zhang J, Liu J, Xu X, Li L. Curcumin suppresses cisplatin resistance development partly via modulating extracellular vesicle-mediated transfer of MEG3 and miR-214 in ovarian cancer. Cancer Chemother Pharmacol. 2017;79(3):479-87.
31. Jiang P, Xu H, Xu C, Chen A, Chen L, Zhou M, et al. NEAT1 contributes to the CSC-like traits of A549/CDDP cells via activating Wnt signaling pathway. Chem Biol Interact. 2018;296:154-61.
32. Cheng H, Sharen G, Wang Z, Zhou J. LncRNA UCA1 Enhances Cisplatin Resistance by Regulating CYP1B1-mediated Apoptosis via miR-513a-3p in Human Gastric Cancer. Cancer Manag Res. 2021;13:367-77.
33. Yuan L, Xu ZY, Ruan SM, Mo S, Qin JJ, Cheng XD. Long non-coding RNAs towards precision medicine in gastric cancer: early diagnosis, treatment, and drug resistance. Mol Cancer. 2020;19(1):96.
34. Gao B, Shao Q, Choudhry H, Marcus V, Dong K, Ragoussis J, et al. Weighted gene co-expression network analysis of colorectal cancer liver metastasis genome sequencing data and screening of anti-metastasis drugs. Int J Oncol. 2016;49(3):1108-18.
35. Bakhtiarizadeh MR, Hosseinpour B, Shahhoseini M, Korte A, Gifani P. Weighted Gene Co-expression Network Analysis of Endometriosis and Identification of Functional Modules Associated With Its Main Hallmarks. Front Genet. 2018;9:453.
36. Schmitt AM, Chang HY. Long Noncoding RNAs in Cancer Pathways. Cancer Cell. 2016;29(4):452-63.
37. Zhu KP, Zhang CL, Ma XL, Hu JP, Cai T, Zhang L. Analyzing the Interactions of mRNAs and ncRNAs to Predict Competing Endogenous RNA Networks in Osteosarcoma Chemo-Resistance. Mol Ther. 2019;27(3):518-30.

38. Wu X, Sui Z, Zhang H, Wang Y, Yu Z. Integrated Analysis of lncRNA-Mediated ceRNA Network in Lung Adenocarcinoma. Front Oncol. 2020;10:554759.

Figures

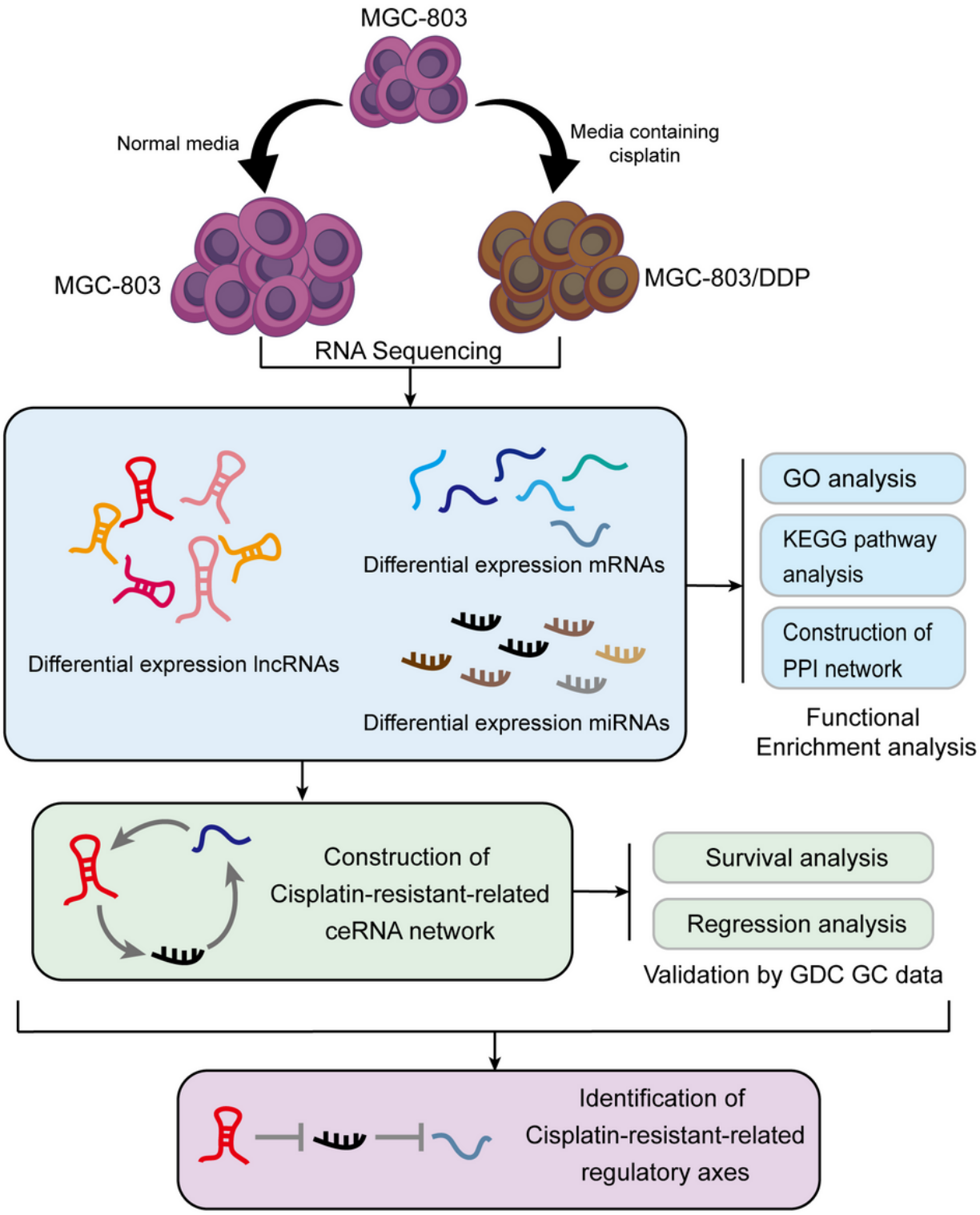

Figure 1

The workflow of this study design. The cisplatin-resistant GC cell line MGC-803/DDP was generated in a stepwise manner by exposing MCG803 cells to intermittently increasing doses of cisplatin (DDP). Total RNA was isolated from MGC-803 and MGC-803/DDP cells for RNA-seq analysis. Gene ontology (GO), KEGG pathway enrichment analysis and the construction of protein-protein interaction (PPI) networks were performed to identify the potential function of differentially expressed (DE) genes. The cisplatin-resistant-related ceRNA network was constructed by bioinformatic analysis. Survival and regression analysis from GDC GC dataset were used to validate our ceRNA network and identify the potential cisplatin-resistant-related regulatory axes.

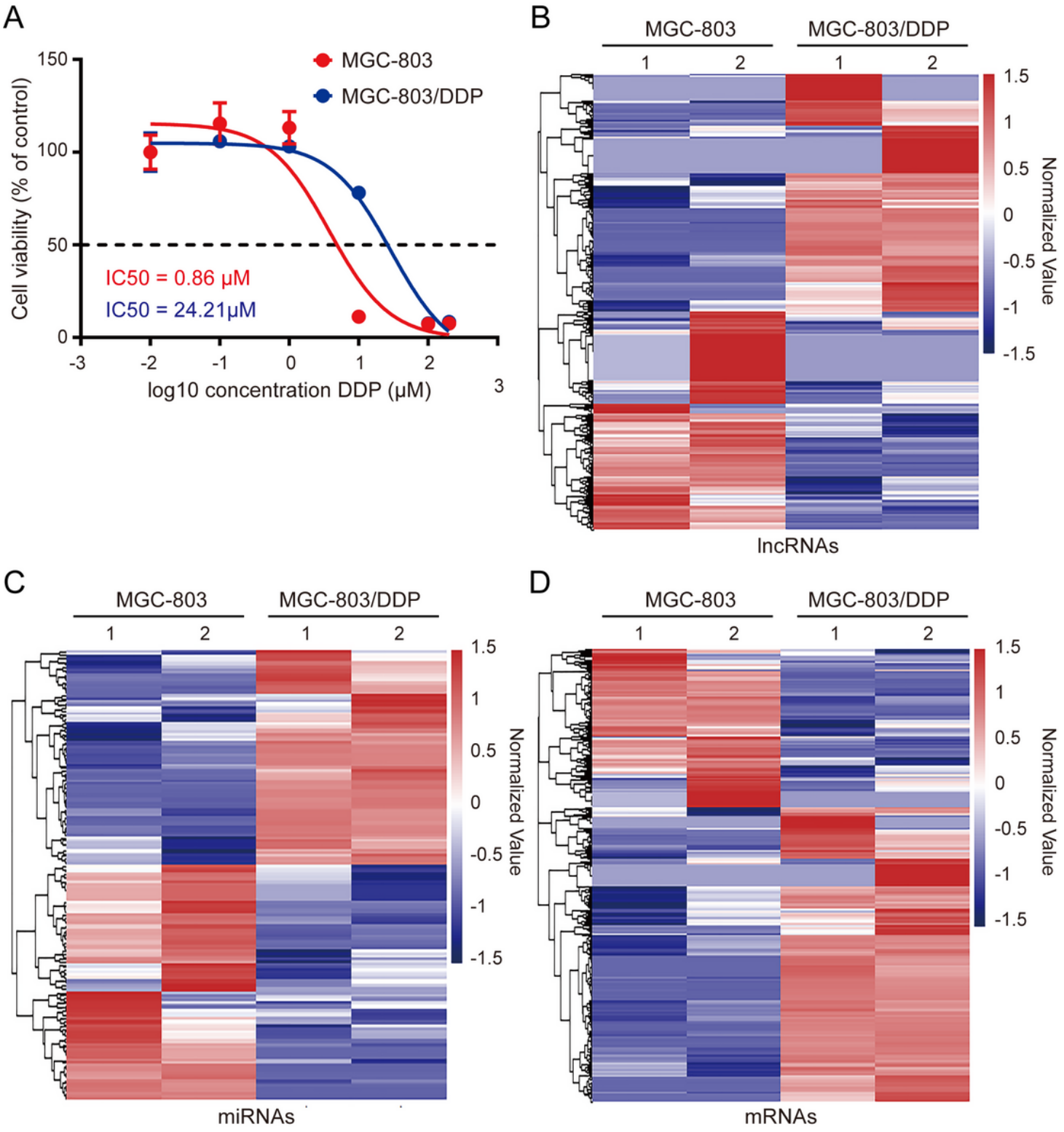

Figure 2

Identification of differentially expressed lncRNAs, miRNAs and mRNAs in MGC-803 and cisplatin-resistant GC cell line MGC-803/DDP. a CCK8 assay of MGC-803 and MGC-803/DDP cells with cisplatin treatment at the indicated concentration for 48 hours. Hierarchical clustering analysis showed all differentially expressed lncRNAs b, miRNAs c, and mRNAs d. Red represents relative upregulation and blue represents relative downregulation.

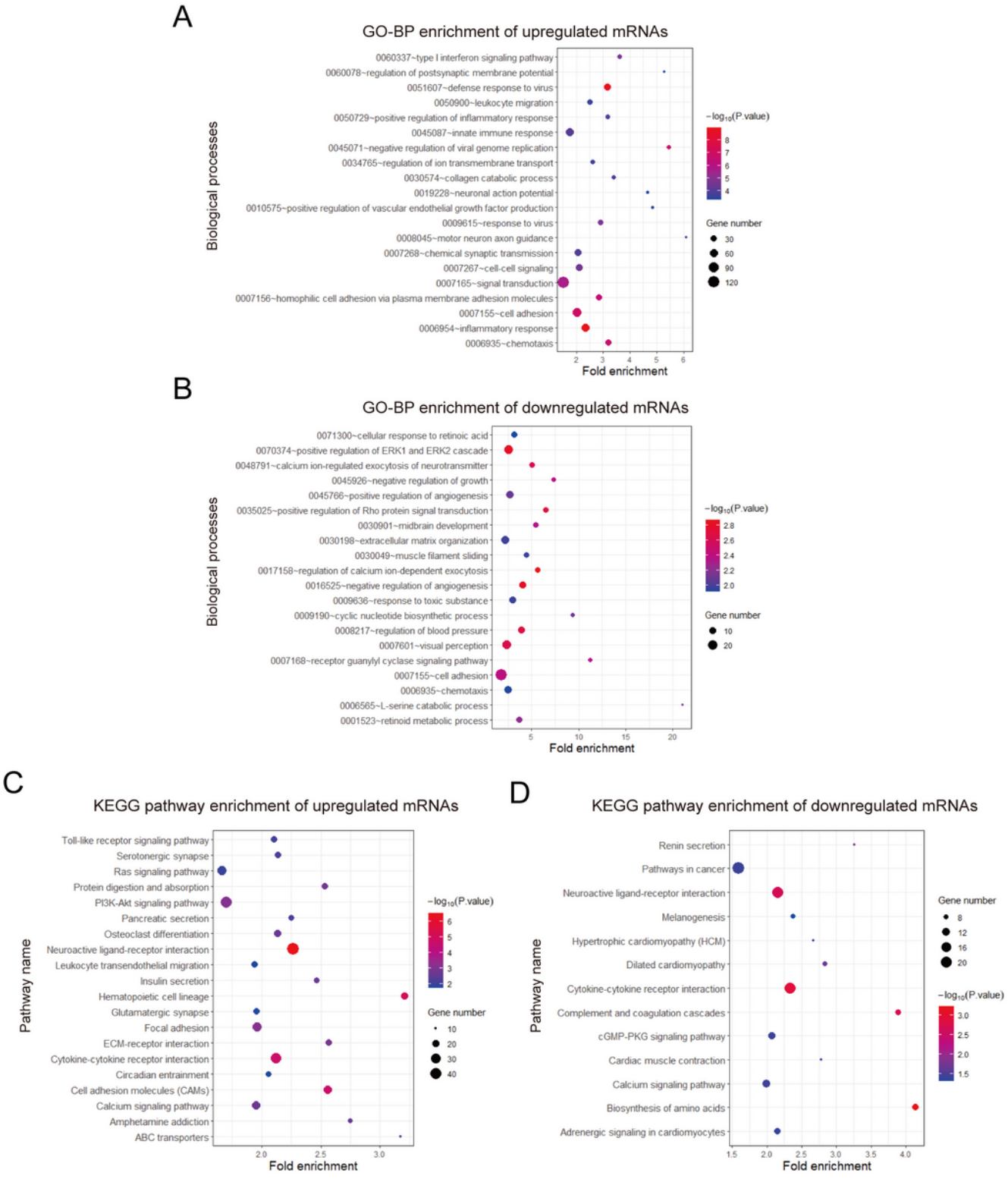

Figure 3

Gene ontology biological process (GO-BP) functional and KEGG pathway analysis of the differentially expressed mRNAs. GO functional analysis of the top 20 biological processes of upregulated mRNAs a and downregulated mRNAs b. KEGG pathway analysis of the top 20 pathways of upregulated mRNAs c and downregulated mRNAs d.

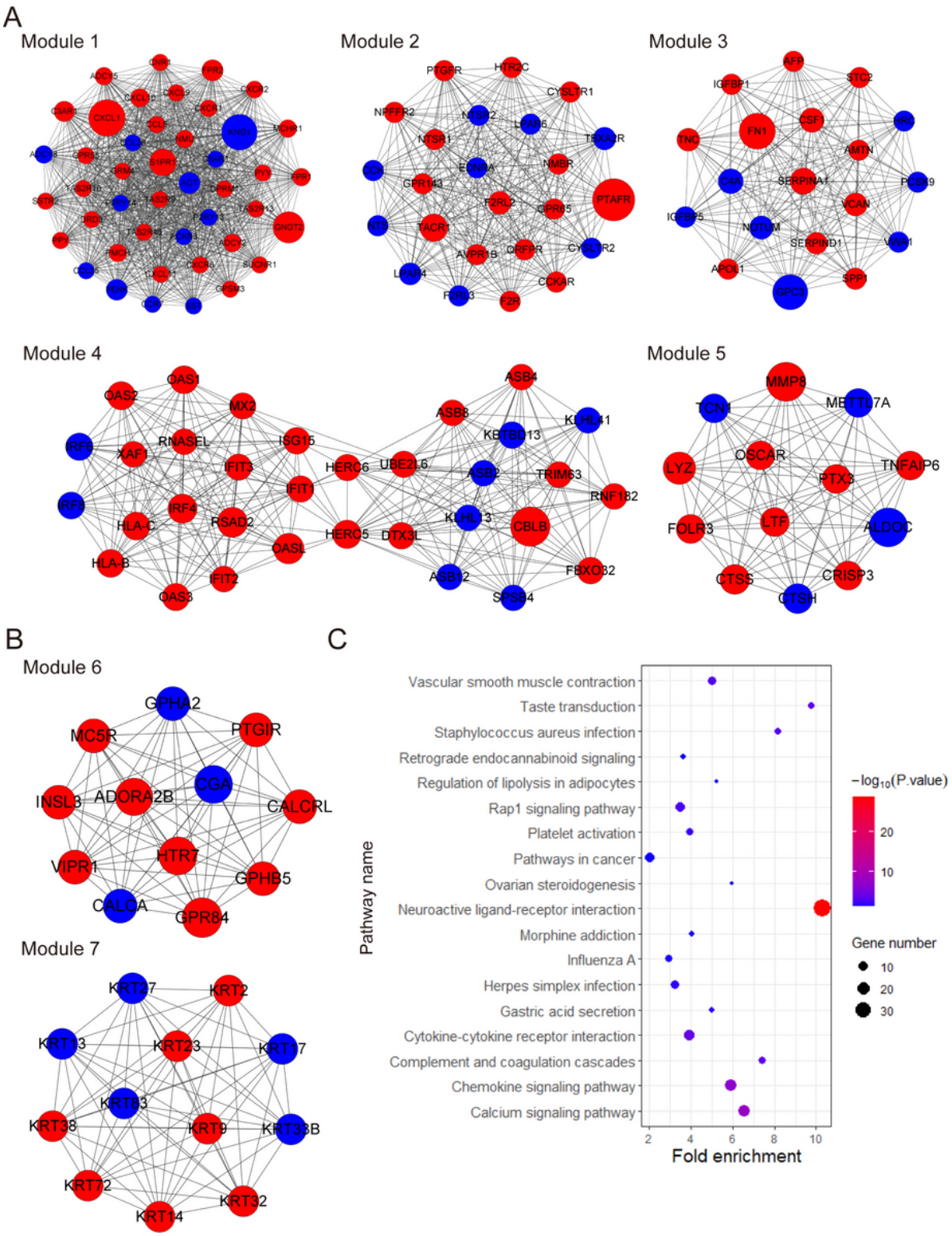

Figure 4

Modules extracted from protein-protein interaction (PPI) network and KEGG pathway analysis of DEmRNAs from these modules. a, b Seven modules extracted from the PPI network. Red and blue circles represent up-and down-regulated DEmRNAs respectively. The size of a node indicated the degree (number of interactions) of the node in the PPI network. c The 18 enriched KEGG pathways of DEmRNAs in these seven modules.

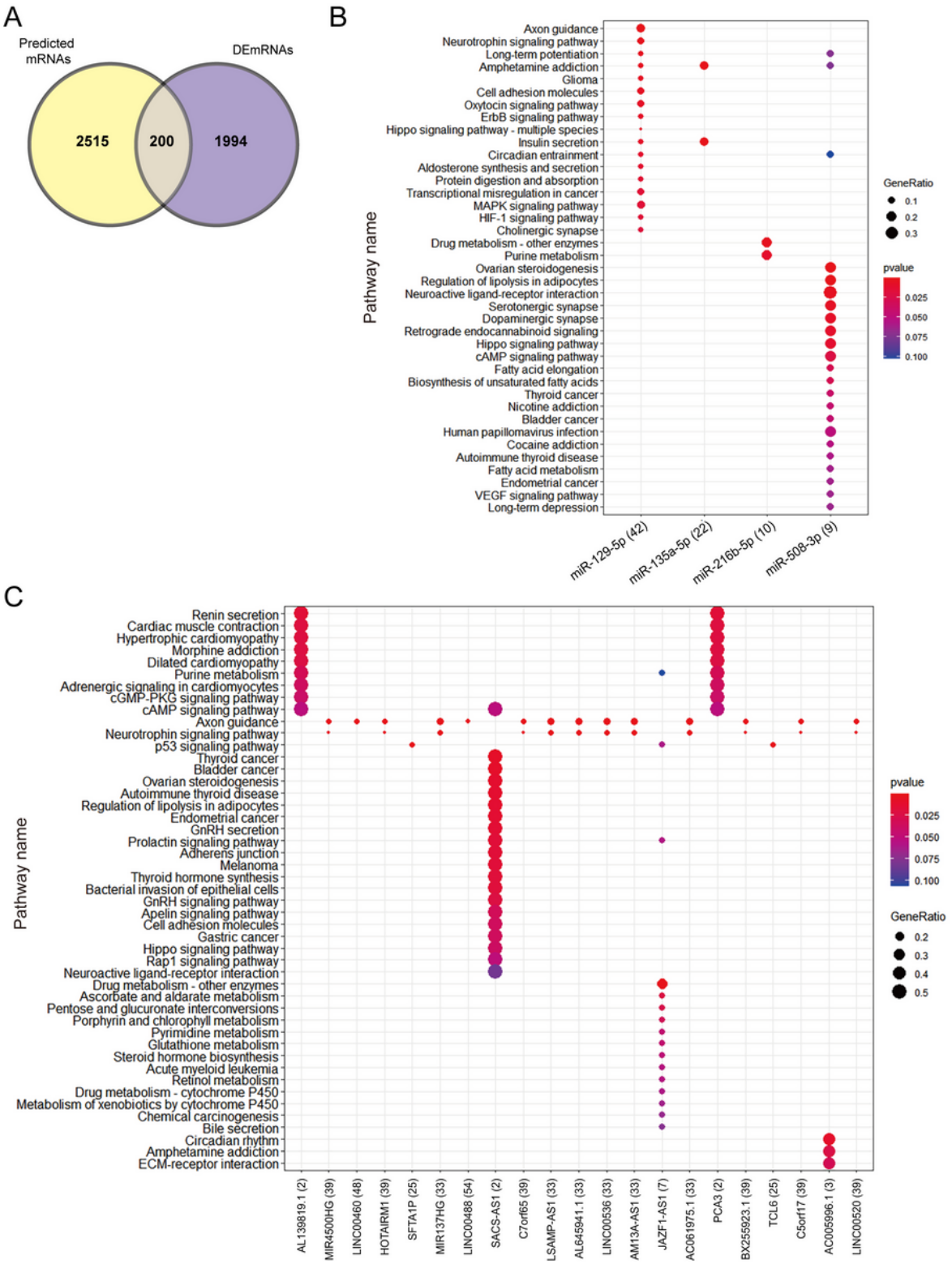

Figure 5

Bubble map of KEGG pathway analysis of DEmiRNAs and DElncRNAs. a Venn diagrams represent the intersections of differentially expressed mRNAs in publicly profile datasets and RNA-seq data. KEGG pathways are enriched by genes regulated by DEmiRNAs b and by DElncRNAs c.

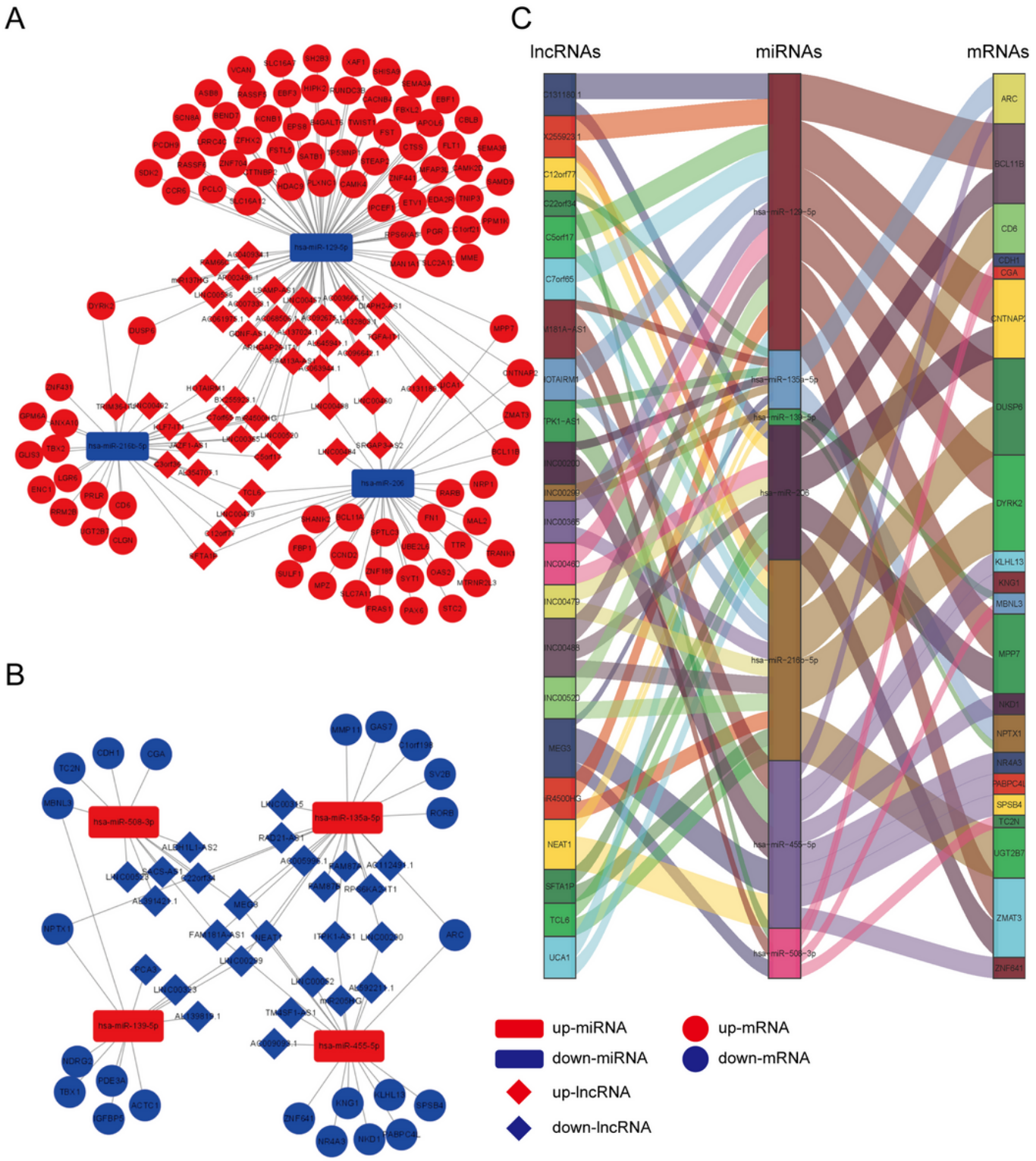

Figure 6

Construction of cisplatin-resistant-related ceRNA network by integrated analysis. a, b Overview of cisplatin-resistant-related ceRNA network. Red nodes were defined as upregulated genes, and blue nodes were defined as downregulated genes. Round rectangle, diamond and circle represent miRNAs, lncRNAs and mRNAs, respectively. c lncRNA-miRNA-mRNA regulatory axes extracted from this ceRNA network.

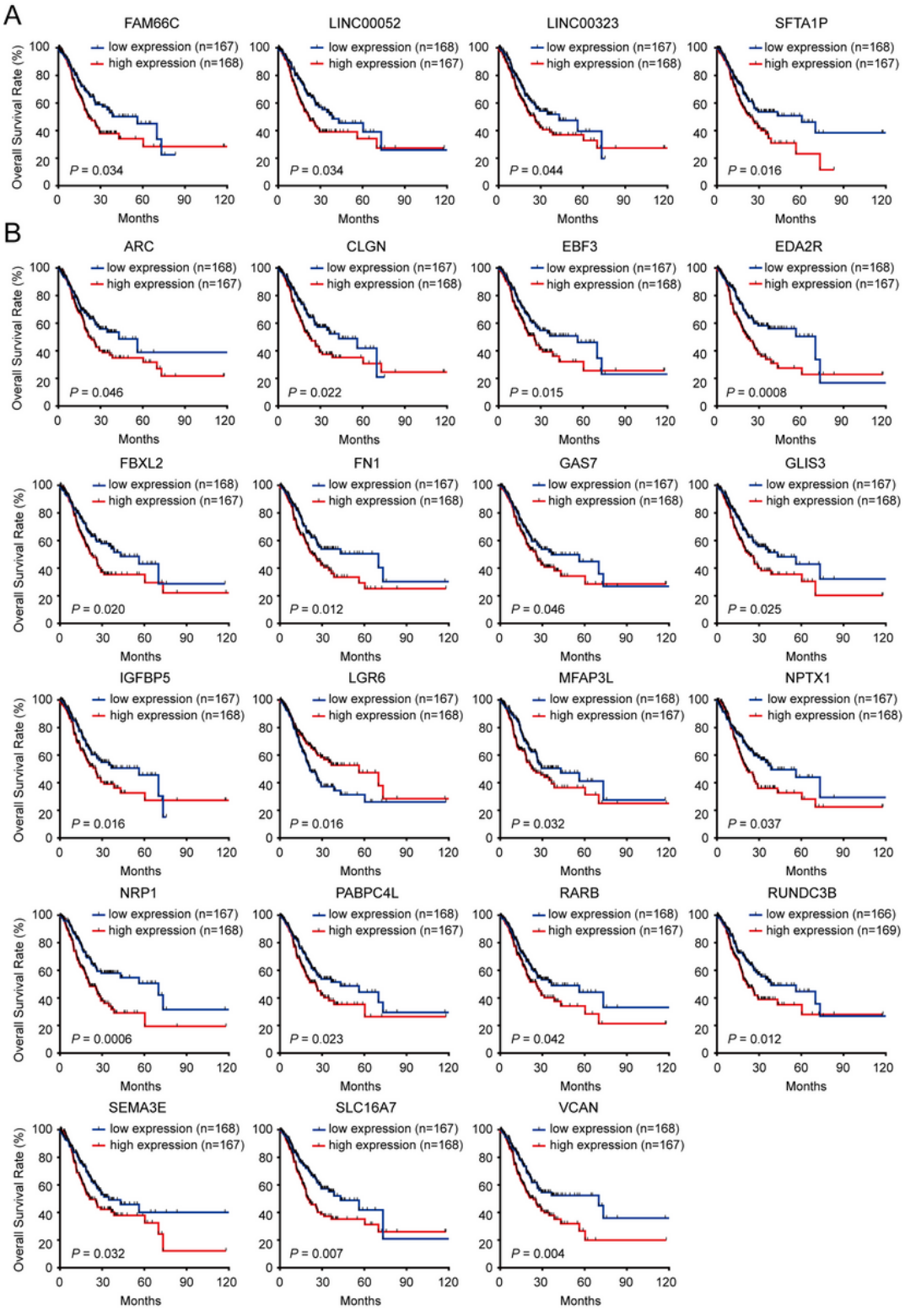

Figure 7

Kaplan-Meier survival analysis of hub DElncRNAs and DEmRNAs from GDC gastric cancer samples. The Kaplan-Meier curve of hub lncRNAs a and mRNAs b that significantly associated with overall survival (OS) in GC patients based on their optimal cutoffs.

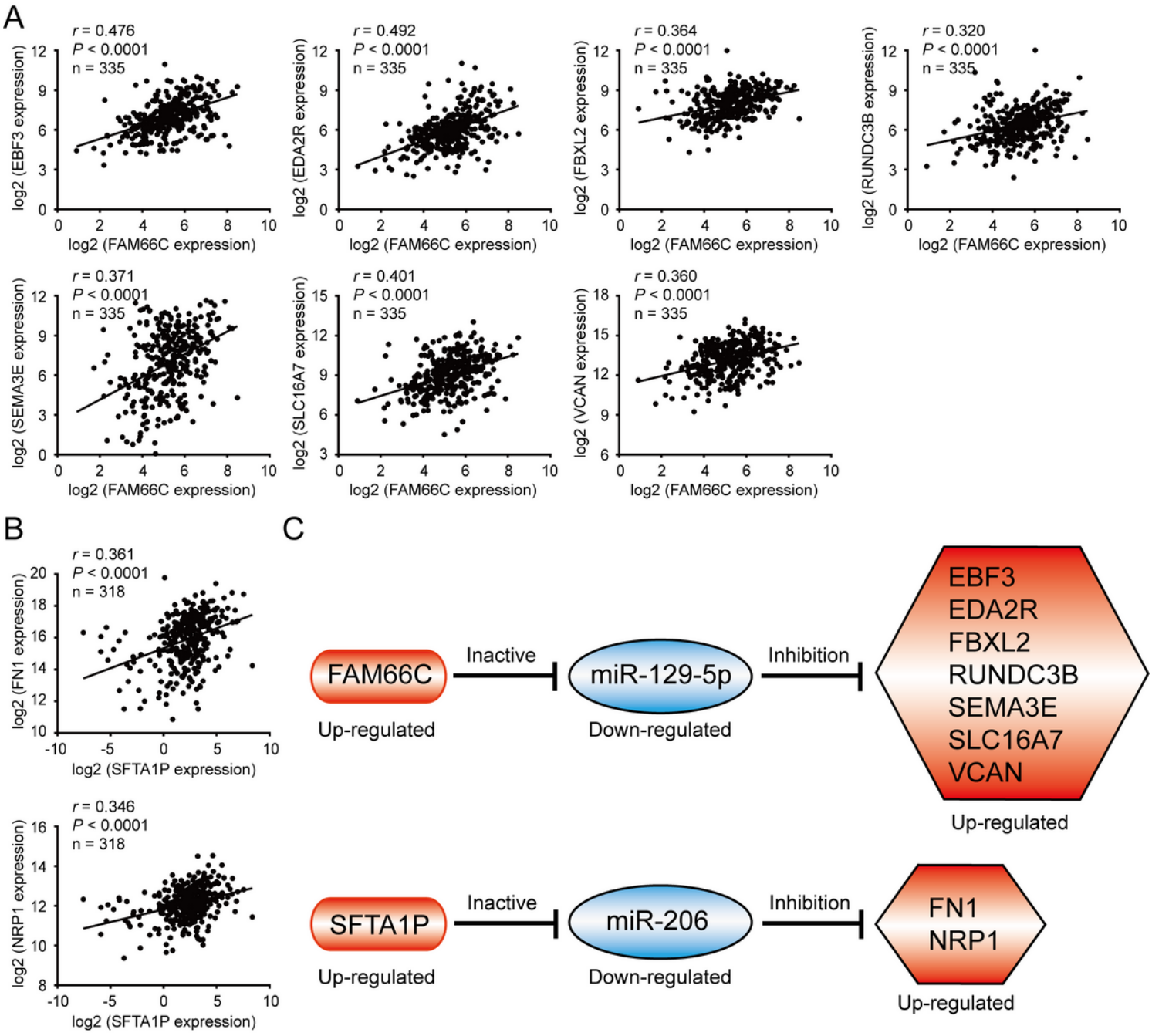

Figure 8

Identification of cisplatin-resistant-related regulatory axes in gastric cancer. a Correlation analysis between FAM66C and seven mRNAs (EBF3, EDA2R, FBXL2, RUNDC3B, SEMA3E, SLC16A7 and VCAN). b Correlation analysis between SFTA1P and two mRNAs (FN1 and NRP1). c The FAM66C/miR-129-5p/7 mRNAs and SFTA1P/miR-206/FN1 or NRP1 regulatory axes perfectly conformed to the ceRNA hypothesis.